

ROCKET ENGINE HEALTH MONITORING USING A MODEL-BASED APPROACH

John P. Butas
NASA Marshall Space Flight Center
MSFC, AL

Claudia M. Meyer
NASA Glenn Research Center
Cleveland, OH

Louis M. Santi
Christian Brothers University
Memphis, TN

T. Shane Sowers
Analex Corporation at NASA Glenn Research Center
Brook Park, OH

Abstract

A stable, accurate and computationally efficient strategy termed Generalized Data Reduction (GDR) was recently developed to support rocket engine analysis. The GDR technique is suitable for the simultaneous real-time estimation of numerous rocket engine health parameters. As such, it has the potential to serve as the foundation for both real-time and post-test/flight rocket engine health monitoring. The previously proposed algorithm has been extended and extensively tested using MC-1 test data. Excellent agreement is shown between GDR and conventional post-test data reduction results for these test data. Results of simulated anomaly studies are presented to demonstrate GDR's ability to identify the causal source of small-scale anomalies. Likewise, the robust response of GDR to missing sensor data is shown through simulated sensor elimination results. Finally, the efficacy of the GDR approach with a small flight-like sensor suite is demonstrated.

Introduction

Monitoring the health of rocket engine systems

Copyright © 2001 by the American Institute of Aeronautics and Astronautics, Inc. No copyright is asserted in the United States under Title 17, U.S. Code. The U.S. Government has a royalty-free license to exercise all rights under the copyright claimed herein for Government Purposes. All other rights are reserved by the copyright owner.

is essentially a two phase process. The acquisition phase involves sensing physical conditions at selected locations, converting physical input to electrical signals, conditioning the signals as appropriate to establish scale or filter interference, and recording results in an easy to interpret form. The inference phase involves analysis of results from the acquisition phase, comparison of analysis results to established health measures, and assessment of health indications.

A variety of analytical schemes can be employed in the inference phase of health monitoring. These schemes can be categorized as statistical, model-based, and rule-based. Statistical analysis methods can provide excellent comparative measures of engine operating health. They generally require well-characterized data from an ensemble of "typical" engines, or "golden" data from a specific test assumed to define the operating norm, in order to establish reliable comparative measures. Statistical methods are generally suitable for real-time health monitoring because they do not deal with the physical complexities of engine operation. The utility of statistical methods in rocket engine health monitoring is hindered by practical limits on the quantity and quality of available data. This is due to the difficulty and high cost of data acquisition, the limited number of available test engines, and the problem of simulating flight conditions in ground test facilities. In addition, statistical methods incur a penalty for

disregarding flow complexity and are therefore limited in their ability to define performance shift causality.

Rule-based methods infer the health state of the engine system based on comparison of individual measurements or combinations of measurements with defined health norms or rules. This does not mean that rule-based methods are necessarily simple. Although binary yes-no health assessments can sometimes be established by relatively simple rules, the causality assignment needed for refined health monitoring often requires an exceptionally complex rule base involving complicated logical maps. Structuring the rule-based system to be clear and unambiguous can be quite difficult, and the expert input required to establish and maintain a large logic network and associated rule base can be prohibitive.

Model-based methods incorporate physical relations and empiricisms in the inference phase of health monitoring. Such methods are typically more involved because the flow physics of rocket engines is generally described by complex, highly interdependent, nonlinear relations. The attending computational complexity may present an impediment to the use of certain model-based methods in real-time health monitoring. However, the addition of physical detail does provide a basis for determining performance shift causality at the component level.

In this paper we describe a model-based method identified as Generalized Data Reduction (GDR) which has been developed for the inference phase of health monitoring. At the highest level, GDR can be considered a strategy for solving the inverse performance analysis problem often referred to as data reduction. More specifically, the method employs a canonical representation of the engine system performance model to estimate the operating characteristics of hardware components such as pumps, turbines, injectors, and orifices consistent with test data. Computational economy provided by the simplified performance representation establishes GDR as a real-time health monitoring tool.

Results of extensive computational experience with the GDR procedure applied to MC-1 (formerly known as Fastrac) engine data are reported. Data from a recent series of MC-1

engine tests conducted at Rocketdyne's Santa Susana test facility are used in this investigation of GDR capability. Comparisons of GDR hardware predictions with those of the parent engine system performance model are presented. These results are used to assess fidelity loss associated with the simplified representation of the parent model used by GDR. The ability of GDR to recover simulated anomalies is demonstrated, information loss associated with single sensor failures is described, and GDR modifications to improve hardware recovery with specific sensor failures are outlined. To better assess flight health monitoring capability, GDR hardware recovery results using a restricted flight measurement set are presented. Computational results from a GDR refinement that employs engine acceptance test information to augment flight measurements is also described.

Generalized Data Reduction

In order to establish a logical context for data reduction, it is important to begin with a general description of rocket engine performance analysis. The objective of performance analysis is to predict engine system operating conditions, **P**, for a specific control state, **C**, using mathematical models of both physical and empirical relations, **F**. Standard engineering models of hardware function within an engine typically contain a number of fixed parameters, **H**, whose values are estimated from accumulated test experience. The set of operating conditions, **P**, includes temperatures, pressures, and flows at defined locations within the engine system. The control state, **C**, of an engine is defined by commanded hardware settings such as valve positions, as well as flow field conditions at the system boundaries.

Performance Analysis Problem

Find **P** such that

$$\mathbf{F}(\mathbf{P}; \mathbf{C}, \mathbf{H}) = \mathbf{0} \quad (1)$$

F set of physical and empirical relations

P set of physical conditions

C set of system control and boundary settings

H set of hardware parameters

For a specific engine system, performance model predictions for the operating conditions, **P**, seldom agree precisely with measured values of

these parameters. Model calibration enforces agreement. To describe the calibration process, termed data reduction, it is convenient to first define the following operating condition and hardware parameter partitions:

$$\mathbf{P} = \{\mathbf{P}_m, \mathbf{P}_t\} \quad \mathbf{H} = \{\mathbf{H}_a, \mathbf{H}_f\} \quad (2)$$

\mathbf{P}_m modeled physical conditions
 \mathbf{P}_t test measured physical conditions
 \mathbf{H}_a adjustable hardware parameters
 \mathbf{H}_f fixed hardware parameters

In order to tune the performance model for a specific engine configuration, \mathbf{H}_a values are adjusted to attain model agreement with the most current test data \mathbf{T} for the selected physical parameters \mathbf{P}_t . The conventional method for effecting this agreement is to solve for the operating conditions \mathbf{P} and hardware adjustments \mathbf{H}_a simultaneously, effectively coupling the performance prediction and data reduction processes. The coupled data reduction problem is described in detail in reference [1]. The linearized decoupled data reduction problem is described below.

Linear Decoupled Data Reduction Problem

Determine \mathbf{H}_a such that

$$\mathbf{F}_c(\mathbf{H}_a; \mathbf{P}_t, \mathbf{C}) = \mathbf{P}_t - \mathbf{P}_{to} - \mathbf{J}_{Hao}(\mathbf{H}_a - \mathbf{H}_{ao}) - \mathbf{J}_{Co}(\mathbf{C} - \mathbf{C}_o) = \mathbf{0}$$

$$\mathbf{P}_t = \mathbf{T}$$

or equivalently

$$\mathbf{T} - \mathbf{P}_{to} = \mathbf{J}_{Hao}(\mathbf{H}_a - \mathbf{H}_{ao}) + \mathbf{J}_{Co}(\mathbf{C} - \mathbf{C}_o) \quad (3)$$

where

$$\mathbf{J}_{Hao} = \left[\frac{\partial \mathbf{P}_{ti}}{\partial \mathbf{H}_{aj}} \right]_0 \quad \mathbf{J}_{Co} = \left[\frac{\partial \mathbf{P}_{ti}}{\partial \mathbf{C}_j} \right]_0$$

\mathbf{J}_{Hao} Jacobian of \mathbf{P}_t with respect to \mathbf{H}_a at base state o

\mathbf{J}_{Co} Jacobian of \mathbf{P}_t with respect to \mathbf{C} at base state o

\mathbf{H}_{ao} and \mathbf{C}_o represent values of the adjustable hardware characteristics and control conditions at a defined base state typical of engine operation. \mathbf{P}_{to} is the performance model solution for the measured parameters at the base conditions. The Jacobian matrices \mathbf{J}_{Hao} and \mathbf{J}_{Co}

are composed of the first order influences of the adjustable hardware and control settings respectively. Performance model simulation results are used to derive finite difference approximations of the appropriate partial derivatives at the base state; these partial derivatives establish the entries in the influence matrices. A detailed description of the GDR development strategy, including the subset selection process which systematically eliminates parameter redundancy, is given in reference [1].

A natural row partition of equation system (3) is defined by the measurements selected for use in data reduction. The reduced form of equation system (3), using only selected measurements s , takes the form below:

$$\mathbf{T}_s - \mathbf{P}_{tso} = \mathbf{J}_{Hso}(\mathbf{H}_a - \mathbf{H}_{ao}) + \mathbf{J}_{Cso}(\mathbf{C} - \mathbf{C}_o) \quad (4)$$

In this relation, $\mathbf{T}_s - \mathbf{P}_{tso}$ represents the difference between test data and computed values for the set of measurement parameters retained by the subset selection process. Equation system (4) is solved for the adjustable hardware characteristics \mathbf{H}_a to complete the data reduction process.

There is generally an infinite number of candidate solutions to the underdetermined system described in equation (4); therefore, a closure principle must be adopted to identify the most appropriate solution. Since the performance model contains the condensed archive of test experience, it is logical to assume that the most likely operating state of the engine will require the smallest shift in hardware state consistent with observation. This provides an effective closure principle and suggests a data reduction formulation based on the optimization problem identified below.

GDR Optimization Problem

GDR optimization involves minimizing

$$(\Delta \mathbf{H}_a)^T \mathbf{W} \Delta \mathbf{H}_a$$

by selecting

$$\Delta \mathbf{H}_a = \mathbf{H}_a - \mathbf{H}_{ao} \quad (5)$$

subject to

$$\mathbf{T}_s - \mathbf{P}_{tso} = \mathbf{J}_{Hso}(\mathbf{H}_a - \mathbf{H}_{ao}) + \mathbf{J}_{Cso}(\mathbf{C} - \mathbf{C}_o) = \mathbf{0}$$

The GDR optimization problem is an equality-constrained weighted least squares problem. The user-specified diagonal weighting matrix \mathbf{W} provides a simple mechanism for expert input based on perceived maturity of hardware component modeling. The problem solution specifies baseline hardware shifts with the smallest weighted least squares value consistent with agreement of test data and computed values for a stable set of measured parameters. Efficient quadratic programming strategies as well as full rank SVD methods may be used to solve problems of this type.^{2,3} The reader is referred to reference [1] for a complete outline of the GDR setup and solution processes.

Restrictions imposed by the linearization can be relaxed by considering appropriate combinations of measured parameters, control conditions, and/or hardware characteristics in the reduction process. An extended procedure, based on combinations of parameters, can be described in functional form as follows.

Extended GDR Optimization Problem

Extended GDR optimization involves minimizing

$$(\Delta \mathbf{h})^T \mathbf{W} \Delta \mathbf{h}$$

by selecting

$$\Delta \mathbf{h} = \mathbf{h} - \mathbf{h}_o \quad (6)$$

subject to

$$\mathbf{p}(\mathbf{T}_s) - \mathbf{p}(\mathbf{P}_{iso}) = \mathbf{J}_{ho}(\mathbf{h} - \mathbf{h}_o) + \mathbf{J}_{co}(\mathbf{c} - \mathbf{c}_o) = \mathbf{0}$$

where

$\mathbf{h} = \mathbf{h}(\mathbf{H}_a)$ set of independent functions of adjustable hardware parameters

$\mathbf{p} = \mathbf{p}(\mathbf{P}_{ts})$ set of independent functions of selected measurements

$\mathbf{c} = \mathbf{c}(\mathbf{C})$ set of independent functions of control settings

$\mathbf{J}_{ho} = \left[\frac{\partial \mathbf{p}}{\partial \mathbf{h}_j} \right]_o$ Jacobian of measurement functions \mathbf{p} with respect to hardware functions \mathbf{h} at base state o

$\mathbf{J}_{co} = \left[\frac{\partial \mathbf{p}}{\partial \mathbf{c}_j} \right]_o$ Jacobian of measurement functions \mathbf{p} with respect to control functions \mathbf{c} at base state o

Appropriate selection of the function sets can be used to mitigate computational stability problems and accommodate nonlinear effects. Results presented later in this paper were derived as solutions to the extended GDR optimization problem constructed specifically for the MC-1 engine system.

MC-1 Engine and Analysis Background

The MC-1 engine is a 60,000 lb vacuum thrust, pump-fed liquid fuel rocket engine that was developed by the NASA Marshall Space Flight Center (MSFC).⁴ The engine burns a mixture of RP-1 hydrocarbon fuel and liquid oxygen. Hot gas produced by a gas generator is used to power a turbine that rotates an inline turbopump assembly. The engine uses five fixed orifices to control engine thrust and mixture ratio. These are the gas generator liquid oxidizer orifice, the gas generator RP-1 orifice, the main liquid oxidizer orifice, the main RP-1 orifice, and the turbine exhaust nozzle orifice. The MC-1 engine is intended to be reusable with the exception of the ablative nozzle.

Three series of MC-1 tests were recently conducted on Rocketdyne's Santa Susana Field Laboratory Alfa-1 test stand in California. The R1 series was focused on resolving any issues associated with the new test stand. The R2 and R3 series consisted of tests to calibrate Engine 3 and Engine 5, respectively. Engines 1 and 2 had previously been tested in the horizontal test facility at the NASA Stennis Space Center (SSC), and Engine 3 had previously been tested at the Propulsion Test Article Facility at SSC. The R2 series used a 15:1 area ratio nozzle and the R3 series used a 30:1 area ratio nozzle; both series were conducted at test stand altitude. Due to separated flow effects inherent in the R3 series tests, only R2 series data sets were utilized in this study. The R2 series consisted of 5 mainstage tests; the first four – R2-1, R2-2, R2-3a and R2-3b – were 24 seconds in duration, and the final test – R2-4 – was a full duration test of 159 seconds.

The tests had varying objectives.⁵ R2-1 established an engine calibration baseline. R2-2

investigated the effect of LOX inlet pressure variations on pump run characteristics. R2-3a was intended to evaluate engine calibration in response to an orifice change; however, due to a leak in the oxidizer bleed valve, this was not accomplished until test R2-3b. Finally, R2-4 was intended to assess engine calibration during full duration (159 seconds) test. The turbine exhaust nozzle orifice was not changed during the R2 series. All other orifices were changed after tests R2-2 and R2-3b. Therefore, tests R2-1 and R2-2 contained identical orifice configurations, as did tests R2-3a and R2-3b.

A ROCETS⁶ performance model of the MC-1 engine was developed at MSFC to support engine design and testing. Fluid conditions in all of the major engine components and flow ducts were modeled using one-dimensional flow physics and empiricisms. This model is the simulation platform used to generate the engine system influence matrices for GDR analyses. In addition, a modified form of this performance model provided the conventional data reduction results used to assess the quality of GDR predictions.

For computational testing of the GDR strategy, a total of 25 engine measurements, corresponding to performance model variables, was employed. These measurements, and their associated model variable names, are given in Table 1. They include four engine inlet condition measurements and 21 internal engine measurements. Included in the measurements list are fourteen pressures, seven temperatures, two flows, one turbopump shaft speed, and one engine thrust. A total of 17 hardware parameters was selected for use in GDR analyses. These 17 hardware characteristics, also given in Table 1, were based on those employed to perform conventional data reduction analyses. Included are six duct/line resistances, four injector resistances, two pump head coefficient multipliers, and one each heat transfer rate, combustion efficiency, nozzle discharge coefficient, orifice discharge coefficient, and turbopump power factor. These engine characteristics 1) are easily derived from the parameter set used for conventional post-test

data reduction, 2) allow systematic incorporation of nonlinear effects in a form appropriate for the extended GDR optimization problem described in the previous section and 3) lead to enhanced computational stability.

All of the hardware parameters described in Table 1 are standard engine parameters, with the exception of the power factor term, PWRFACT. The power factor provides a measure of the discrepancy between the standard turbopump efficiency computed from performance model maps, and the actual turbopump efficiency indicated by test data. Use of the power factor instead of individual pump and turbine efficiencies was motivated by both uncertainty and stability considerations.

All of the measurements indicated in Table 1 would not typically be available on a flight engine. As part of the former X-34 program, for example, the MC-1 engine was expected to have only the following sensors: the liquid oxidizer pump discharge pressure, the RP-1 pump discharge pressure, the main chamber pressure, the turbine inlet pressure and the turbine inlet temperature. Engine inlet temperatures and pressures would be provided as part of the vehicle main propulsion system data. With such a reduced measurement list, the estimable hardware parameters would require consolidation. The reduced hardware set used for flight engine analyses includes ECSMMCHB, PSIMOPMP, PSIMKPMP and PWRFACT from the original set in Table 1, as well as new hardware parameter combinations defined in Table 2.

Results

In order to assess the potential of the GDR strategy for a health monitoring (HM) application, it is necessary to examine reduction results for accuracy, computational efficiency, reliability, and anomaly detection capability. An investigation of GDR suitability for HM was conducted using R2 series data from the MC-1 engine test program.

	Physical Measurements		Hardware Parameters
	Engine Inlet		Oxidizer System
1	Engine LOX Inlet P (PSVL10)		
2	Engine LOX Inlet T (TTVL10)	1	LOX Pump Head Coefficient Multiplier (PSIMOPMP)
3	Engine RP-1 Inlet P (PSRPFV)	2	Main LOX Duct Resistance (RMMCOX)
4	Engine RP-1 Inlet T (TTRPFV)	3	Main LOX Injector Inlet Duct Resistance (ROLN1)
	Fuel System	4	Main LOX Injector Resistance (ROINJ)
1	RP-1 Pump Inlet P (PSVL00)	5	GG LOX Line Resistance (RMGGOX)
2	RP-1 Flowrate (WRPTOTL)	6	GG LOX Injector Resistance (RGGOI)
3	RP-1 Pump Discharge P (PSVL01)	7	GG LOX Flow Heat Transfer (QDOTVL18)
4	RP-1 GG Inlet P (PSVL09)		Fuel System
5	RP-1 Manifold P (PTVL05)	8	Fuel Pump Head Coefficient Multiplier (PSIMKPMP)
6	RP-1 Manifold T (TTVL05) *	9	RP-1 Pump Inlet Duct Resistance (RKFL1)
	Oxidizer System	10	Main Fuel Line Resistance (RMMCRP)
7	LOX Pump Discharge P (PSOXDS)	11	Main Fuel Injector Resistance (RKINJ)
8	LOX Flowrate (WOXTOTL)	12	GG RP-1 Line Resistance (RMGGRP)
9	Main OX Line Intermediate P (PSVL13)	13	GG RP-1 Injector Resistance (RGGKI)
10	GGOV Inlet Pressure (PSVL15) *		Turbine/ GG System
11	LOX GG Inlet P (PSVL18)		
12	LOX GG Inlet T (TTVL18)	14	Turbine Exhaust Nozzle Orifice Cd Multiplier (CDGGNZ)
13	LOX Dome P (PTVL14)	15	Turbopump Efficiency Multiplier (PWRFACT)
14	LOX Dome T (TTVL14) *		Main Chamber
	GG/Turbine System		
15	Turbine Inlet T (TTHTGI)	16	Main Chamber c* Efficiency Multiplier (ECSMMCHB)
16	Turbine Inlet P (PTHTGI)	17	Nozzle Cd Multiplier (CDNOZL)
17	Turbine Discharge P (PTVL22)		
18	Turbine Discharge T (TTHTGD) *		
19	Shaft Speed (SNSHFT)		
	Main Chamber		
20	Main Chamber P (PTMCHY)		*not utilized based on subset selection stability criteria
21	Thrust (FT15A)		

Table 1 - Measurements and hardware parameters considered in GDR analyses of MC-1 engine

Flight Hardware Parameter	Definition
R3MCOX	RMMCOX+ROLN1+ROINJ
R3MCRP	RMMCRP+RKINJ
R3GGOX	RMGGOX+RGGOI
R3GGFV	RMGGRP+RGGKI

Table 2 - Flight hardware parameter combinations

Comparison with ROCETS/MC-1 Data Reduction Results

In order to assess the accuracy of GDR results, it is necessary to adopt a standard of comparison. The GDR procedure relies upon a parent performance model to establish the functional relationships between hardware variation and measured parameter changes. Since the parent model currently provides the accepted data reduction results used in post-test review, the data reduction results from this parent model are the de facto standard.

Due to the well-determined system restriction of the conventional data reduction method, only 21 (4 inlet and 17 internal) of the 25 measurements listed in Table 1 were used to derive conventional data reduction results. In addition, the 17 hardware characteristics used in GDR analyses were based on, but not identical to, the 17 hardware parameters estimated by the conventional data reduction method. For comparison purposes, corresponding values of the 17 hardware characteristics used in GDR analyses were computed from conventional model results.

Using measurements from each R2 series test, time history data reductions were performed using both ROCETS-based data reduction and GDR. Although GDR does not have the well-determined system restriction of conventional methods, 17 measurements were also specified for GDR analyses in order to facilitate the comparison between GDR and ROCETS data reduction results. It should be noted that the GDR subset selection procedure eliminated precisely those measurements which were not used in ROCETS data reduction: GGOV Inlet Pressure (PSVL15), RP-1 Manifold Temperature (TTVL05), Turbine Discharge Temperature (TTHTGD), and LOX Dome Temperature (TTVL14). Time history data reduction predictions were derived for each hardware characteristic over a sequence of one-second time slices beginning six seconds after engine ignition and ending at shutdown. One-second average test data were used at each time slice to estimate measurement values. Representative reduction results derived from R2-4 test data are displayed in Figures 1 and 2.

Figure 1 shows that the ROCETS data reduction and GDR predictions for the LOX pump head coefficient multiplier, PSIMOPMP, are virtually identical over the entire 154 second interval. Discernable, although extremely small, differences between predictions of the two methods for the R2-4 main chamber c* efficiency multiplier, ECSMMCHB, are seen in Figure 2. Uniformly good agreement between predictions of the two methods was observed for all 17 hardware characteristics over all R2 series tests.

Table 3 contains a summary of the average absolute error for each of the seventeen hardware characteristics over each of the R2 series tests. The excellent overall level of agreement between

GDR predictions and ROCETS data reduction results is apparent. Only one hardware parameter, the fuel pump inlet duct resistance RKFL1, displayed a difference of over 1%, and then only for test R2-1. Only three instances of a test average absolute difference above 0.5% were observed.

Having established that GDR can provide an acceptable level of accuracy for MC-1 engine data reduction, it was also important to verify that GDR computational efficiency is consistent with real-time HM requirements. The clock time required to read the 21 measurements for a particular time slice and perform a complete GDR analysis to recover the 17 named hardware characteristics was measured using data from test R2-4. The clock time required to perform 154 (one for each 1-second time slice) such reduction cycles in sequence using a PC-based computer system with an 800 MHz Pentium III processor was found to be just over one second. Therefore, the single reduction cycle compute time for GDR analysis of the MC-1 engine system using 21 measurements to predict 17 hardware performance characteristics was under 0.01 seconds. This was substantially smaller than the one second monitoring cycle period and served to verify GDR computational efficiency

Hardware Parameter	Average Absolute Error (%)			
	r2-1	r2-2	r2-3b	r2-4
RGGKI	0.036	0.031	0.046	0.056
RGGOI	0.019	0.142	0.019	0.150
RKINJ	0.092	0.126	0.135	0.106
ROINJ	0.044	0.071	0.015	0.024
CDGGNZ	0.002	0.002	0.002	0.017
CDNOZL	0.008	0.031	0.021	0.029
ECSMMCHB	0.017	0.232	0.081	0.059
PSIMKPMP	0.028	0.059	0.026	0.043
PSIMOPMP	0.010	0.015	0.004	0.010
RMMCRP	0.119	0.139	0.149	0.115
RMMCOX	0.042	0.731	0.094	0.136
RKFL1	1.239	0.171	0.227	0.143
ROLN1	0.006	0.037	0.004	0.051
RMGGRP	0.154	0.294	0.092	0.064
RMGGOX	0.046	0.659	0.098	0.093
PWRFACT	0.023	0.018	0.005	0.009
QDOTVL18	0.081	0.086	0.103	0.402

Table 3 - Average absolute GDR error when compared to ROCETS data reduction results

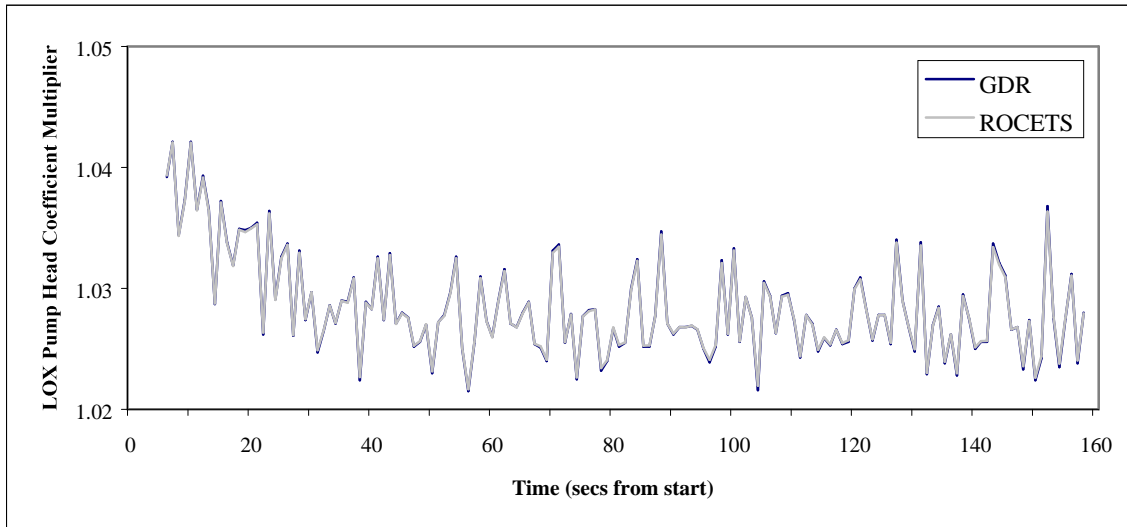


Figure 1 - Test R2-4 comparisons of ROCETS data reduction results and GDR predictions for the LOX pump head coefficient multiplier

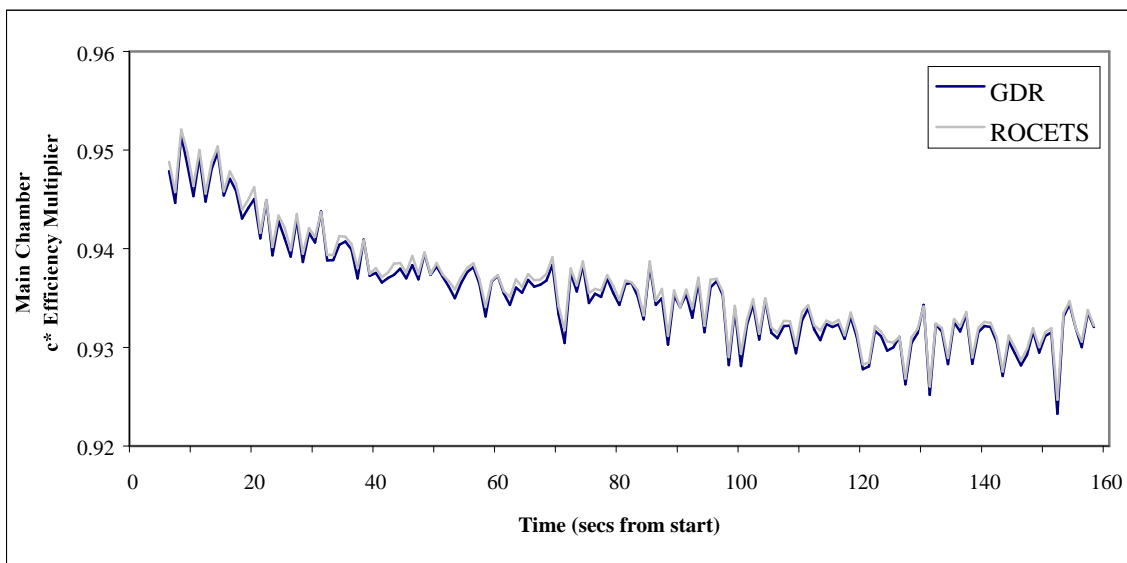


Figure 2 - Test R2-4 comparisons of ROCETS data reduction results and GDR predictions for the main chamber c^* efficiency multiplier

consistent with HM requirements for the MC-1 engine system.

Simulated anomaly recovery

The central capability of any HM system is the detection and isolation of operating anomalies. In the absence of data from an engine system experiencing an actual operating anomaly, the ability to identify simulated failure scenarios provides an appropriate test for a data reduction tool.

In order to assess the ability of GDR to identify operating anomalies, a study of responses to simulated single source anomalies was conducted. To approximate the measurement stream from a single source anomaly, each of the 17 independent hardware characteristics used in reduction studies was individually incremented within the ROCETS/MC-1 performance model to simulate anomalous function of the associated hardware component. For each simulated single source anomaly, the ROCETS/MC-1

performance model then returned predicted values of the 21 measured parameters employed in the reduction process. These values were provided as measurement inputs to GDR. The reduction output was subsequently examined to determine the accuracy of individual source anomaly recovery.

A representative result for the fuel pump head coefficient multiplier, PSIMKPMP, is presented in Figure 3. The performance model inputs used to generate the simulated measurements for GDR were precisely the R2-4 base values, with the exception of PSIMKPMP; PSIMKPMP was set at 95% of its base value. The line in Figure 3 represents GDR predicted values for the 17 hardware parameters, expressed as a fraction of the R2-4 base case values. Note that GDR has assigned hardware causality associated with the anomaly case measurements across all hardware characteristics, with by far the greatest causality correctly assigned to PSIMKPMP.

Table 4 displays the magnitude of the single source anomaly utilized for each hardware parameter, expressed as a percentage of the R2-4 base value for that parameter. In addition, for each of the 17 independent hardware characteristics, the percentage error in the single source anomaly recovery by GDR is displayed. The largest observed discrepancy of 2% occurs for the Main Fuel Line Resistance, RMMCRP. Due to the fact that RMMCRP is actually a combination of performance model hardware parameters, it is not directly perturbed. A related

Hardware Parameter	Perturbation (%)	Error in GDR recovery of perturbed parameter (%)
RGGKI	23.46	0.82
RGGOI	23.46	1.97
RKINJ	23.46	0.95
ROINJ	23.46	0.13
CDGGNZ	-5.00	0.14
CDNOZL	-5.00	0.29
ECSMMCHB	-5.00	0.02
PSIMKPMP	-5.00	0.21
PSIMOPMP	-5.00	0.06
RKFL1	10.00	0.01
ROLN1	10.00	0.02
RMGGRP	23.31	0.34
RMGGOX	23.38	0.70
RMMCRP	29.94	2.19
RMMCOX	19.93	0.07
PWRFACT	-3.25	0.06
QDOTVL18	10.00	0.00

Table 4 - Magnitudes of simulated single source anomalies and errors in GDR recovery of these anomalies

performance model hardware parameter was perturbed by 10%, resulting in a 23.46% increase in this resistance. This large resistance change is accurately predicted by GDR. In general, the GDR recovered value of the anomaly characteristic is within +/-1% of the generating value. This indicates an excellent ability to identify the causal source of small scale anomalies.

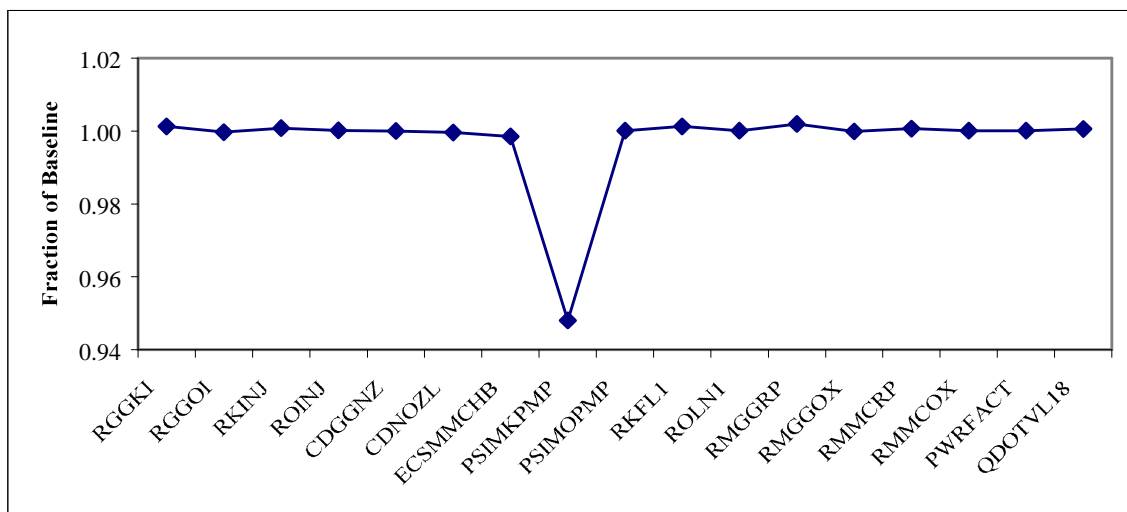


Figure 3 - GDR recovery of PSIMKPMP anomaly

Sensor Elimination Study

A robust HM strategy must be capable of accommodating sensor failures without excessive degradation in the accuracy of engine health assessment. To accomplish this, data from a malfunctioning sensor must first be recognized as emanating from defective instrumentation rather than changes in host system function, and then eliminated from any computational scheme aimed at assessing operational health. Once suspect sensor data have been eliminated, the loss of health monitoring capability must be evaluated, and assessment procedures adjusted to best utilize the remaining data. The comparative tools required for identification of sensor malfunction were not considered as part of this effort. However, the effect of single sensor data loss on the accuracy of GDR results for the MC-1 engine was investigated. Adjustments to the computational procedure that improved the accuracy of reduction results for specific single sensor data loss cases were also identified.

In order to assess the impact of individual sensor failures on GDR predictions of MC-1 engine operation, a simulation study was again performed. Each of the 17 primary internal measurements was individually eliminated from a specific GDR run. In most cases, the measurement set used in the restricted reduction analysis was composed of the remaining sixteen primary internal measurements. For certain sensor loss cases, accuracy of the reduction results was enhanced by considering fewer measurements. The total number of sensors used in performing the final reduction is indicated in Table 5. In all cases where the number is 16, the unused measurements were the failed measurement in question and the typical four measurements eliminated through subset selection – PSVL15, TTVL05, TTHTGD and TTVL14. For the three cases where the final number of measurements used was 15, the recovery accuracy was enhanced when an additional measurement was also eliminated.

For several intermediate duct/line pressures; namely PTVL05, PSVL09, PSVL13, PTVL14, and PSVL18, the loss of sensor data did not impact the overall accuracy of GDR predictions. This is because the loss of sensor data for these

Measure- ment	Number of measure- ments used by GDR	0.5% < error ≤1%	1% < error ≤2%	error > 2%
PSOXDS	16		RMMCOX, RMGGOX	
WOXTOTL	15	ECSMMCHB, PSIMOPMP, ROLN1	ROINJ, RMGGOX	
WRPTOTL	16	RKINJ, RMMCRP	RKFL1	
PSVL00	16			RKFL1
PSVL01	16			RMMCRP, RMGGRP
PTMCHY	16	RKINJ		
PTHTGI	16	RGGKI, RGGOI		
TTHTGI	16	RMGGOX, PWRFACT	RGGKI	RMGGRP
FT15A	16	CDNOZL, ECSMMCHB		
TTVL18	16			
SNSHFT	15			
PTVL22	16	CDGGNZ		

Table 5 - Effect of single sensor data loss on GDR analysis procedure and results

measurements was observed to impact only resistances proximate to the sensor location. A typical case using R2-4 test data is displayed in Figure 4 for the main oxidizer line intermediate pressure, PSVL13. When sensor data for PSVL13 are lost, the primary effect is a reduction in the ability to discriminate between changes in the proximate line resistances RMMCOX and ROLN1. However, when the resistance sum RMMCOX + ROLN1 is examined, the PSVL13-lost and original, full measurement suite ROCETS data reduction results are virtually identical. The impact of the loss of PSVL13 on GDR predictions for other hardware characteristics is negligible. In effect, the loss of PSVL13 has little effect on the accuracy of GDR results as long as the effective resistance sum RMMCOX + ROLN1 is used to replace the component resistances. All 5 intermediate duct/line pressures identified above exhibited similar behavior which could be completely accommodated by resistance combinations.

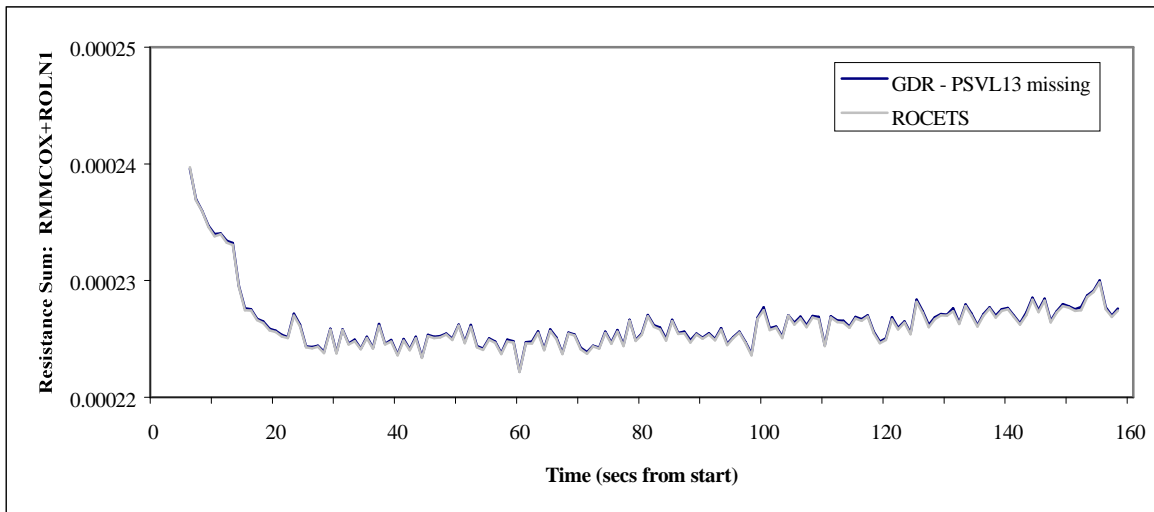


Figure 4 - Behavior of RMMCOX+ROLN1 with and without the loss of sensor measurement PSVL13, the main oxidizer line intermediate pressure

The degradation of GDR accuracy associated with the loss of a single sensor is characterized in Table 5 for all primary MC-1 engine measurements. Loss of predicted hardware fidelity less than 0.5% was considered to be benign. Hardware parameters with errors in excess of 2% were considered problematic and health assessments related to these parameters are not indicated if the associated sensor failure occurs. Health assessments related to parameters with errors between 0.5% and 2% should be carefully considered if the associated sensor failure is identified.

Flight Measurement Set

The ultimate test of an engine health monitoring system occurs during flight operations. Health assessment for a sparsely instrumented flight engine requires robust tools. As indicated previously, only five internal measurements were anticipated for flight-ready MC-1 engines. Because thrust and intermediate pressure indications were to be absent in flight engines, the number of reduction hardware parameters was reduced to eight. This included four of the original hardware set as well as the four resistance combinations presented in Table 2.

It should be observed that using five internal measurements and eight hardware parameters specifies the reduction system as underdetermined. The solution of the extended GDR optimization problem (6) for underdetermined systems is the hardware combination that minimizes the shift away from the base case hardware values in the least squares sense, while enforcing model agreement with test values of the measured parameters. Assuming base state values represent best available estimates for the hardware parameters, the GDR solution can be thought of as a type of maximum likelihood prediction given measured conditions.

In the GDR process, inlet conditions are used to correct the off-baseline shift of measured properties in response to changing inlet propellant properties. One method of augmenting this correction is to treat data from the engine acceptance test in the same manner as inlet properties are used. Since MC-1 engine systems would be expected to undergo brief acceptance testing prior to flight, the availability of acceptance test data for flight operations is assumed. For the MC-1 engine, the use of simulated acceptance test data for the oxygen and RP-1 flow rates, WOXTOTL WRPTOTL, was found to improve certain predictions.

GDR analyses of MC-1 engine operation in test R2-4 were performed using only the five internal measurements and the eight hardware parameters appropriate for flight. Representative results are displayed in Figures 5 and 6. Both figures display standard ROCETS data reduction results using all 17 primary internal measurements and GDR predictions using only flight set measurements. GDR predictions with and without acceptance test information are displayed. For purposes of this study, the acceptance test value for each propellant flow was assumed to be the 20 to 23 second average of the R2-4 test data.

It is obvious from examination of Figure 5 that use of propellant acceptance test information improves both trending and accuracy for the oxygen pump head coefficient multiplier PSIMOPMP. Similar comments are appropriate for the main chamber c^* efficiency multiplier results displayed in Figure 6. The fluctuation of GDR flight reduction results is observed to be muted relative to standard full set predictions, especially when acceptance test propellant flows are used.

Table 6 provides values of the R2-4 average absolute prediction error obtained for each

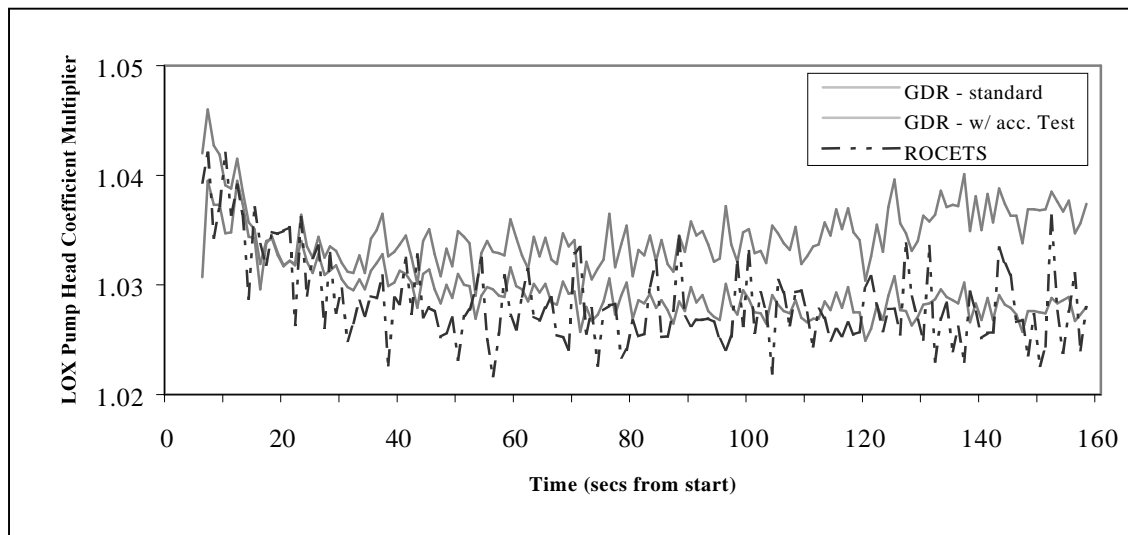


Figure 5 - GDR flight measurement results for the LOX pump head coefficient multiplier - with and without acceptance test information

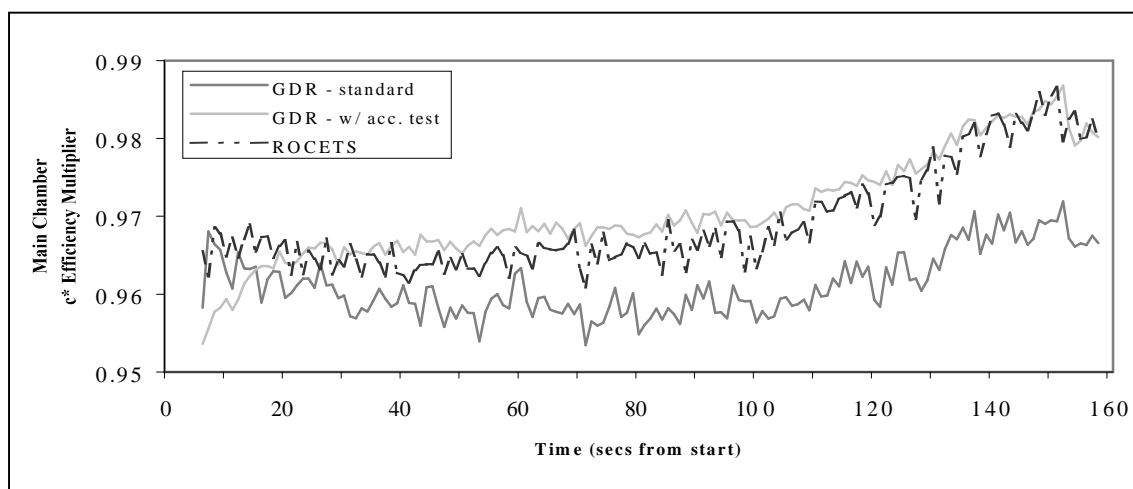


Figure 6 – GDR flight measurement results for the main chamber c^* efficiency multiplier – with and without acceptance test information

Hardware Parameter	Without flow averages from acceptance test		With flow averages from acceptance test	
	Average Absolute Error (%)	Standard Deviation	Average Absolute Error (%)	Standard Deviation
R3MCOX	0.986	0.006	0.303	0.003
R3MCRP	1.100	0.008	1.28	0.005
R3GGOX	0.107	0.001	0.230	0.001
R3GGRP	0.059	0.000	0.0700	0.000
PWRFACT	0.294	0.002	0.612	0.003
ECSMMCHB	0.845	0.004	0.286	0.002
PSIMKPMP	0.270	0.002	0.240	0.002
PSIMOPMP	0.617	0.004	0.287	0.002

Table 6 - GDR accuracy using only flight measurements

hardware parameter. In this case, the average absolute error is defined as the average of the absolute difference between GDR flight set reduction results and ROCETS full set data reduction results. Absolute error values are prescribed for GDR results generated both with and without acceptance test propellant flow information. Using acceptance test flows, only two parameters exhibit an average absolute error above 0.5%, while four have errors exceeding 0.5% without considering these flows. It is also observed in Table 6 that the standard deviation of the absolute error is in general improved using acceptance test flows. Considering the limited number of internal measurements available in flight, these results are considered to be very good.

Summary

The GDR process is a model-based inference tool that is applicable to any system whose performance can be described by physical relations and hardware empiricisms with tunable parameters, such as a rocket engine. It can provide exceptionally fast health information for real-time decision-making by an on-board control system or a control room operator.

For the fixed-orifice MC-1 engine, the results presented in this paper support the use of GDR as a health monitoring tool. The GDR strategy employed had been modified to better account

for system nonlinearity. The introduction of nonlinearity, through the parameter functions described in problem statement (6), preserved the computational efficiency of linearity while improving system stability and accuracy.

GDR results showed excellent agreement with conventional data reduction results. Clear indication of small-scale anomaly recovery was presented, although a more thorough evaluation of this capability would require data from realistic scenarios exhibiting multi-component anomaly operation. Reduction flexibility in the presence of single sensor failures is also indicated. The consequences of multiple simultaneous sensor failures and measurement bias need to be investigated further. For the MC-1 engine system, a small set of flight measurements provided an adequate basis for recovery of pertinent parameters describing hardware function. Flight measurement results were obtained by using an underdetermined system of defining equations and the closure principle defined by the extended GDR optimization problem.

References

1. Santi, L. and Butas, J., "Generalized Data Reduction Strategy for Rocket Engine Applications," AIAA 2000-3306, 36th AIAA/ASME/SAE/ASEE Joint Propulsion Conference and Exhibit, July 2000.
2. Dongarra, J.J.; Du Croz, J.; Duff, I.S. and Hammerling, "Algorithm 679 – A Set of Level 3 Basic Linear Algebra Subprograms," ACM Trans. Math. Soft., Vol. 16, 1990, pp.1-17.
3. Cline, R.E. and Plemmons, R.J., "L₂-Solutions to Underdetermined Linear Systems," SIAM Review, Vol. 18, 1976, pp.1-17.
4. Ballard, Richard O. and Olive, Tim, "Development Status of the NASA MC-1 (Fastrac) Engine, AIAA 2000-3898, 36th AIAA/ASME/SAE/ASEE Joint Propulsion Conference and Exhibit, July 2000.
5. "MC-1 ALFA-1 R2 Test Series Data Review, Engine Systems Section," NASA Marshall Space Flight Center, September 2000.
6. "System Design Specification for the ROCETS (Rocket Engine Transient Simulation) System," Pratt & Whitney FR-20284, prepared for NASA MSFC, August 24, 1990.